p-p Interactions at 2 Bev. II. Multiple-Pion Production*

E. PICKUP,† D. K. ROBINSON, AND E. O. SALANT
Brookhaven National Laboratory, Upton, New York

(Received October 25, 1961)

Analyses have been made for 871 four-prong events and 463 two-prong events corresponding to multiple pion production, resulting from p-p interactions at 2 Bev in the BNL 20-in. hydrogen bubble chamber. Cross sections have been obtained for all the observable double and triple pion production processes; the branching ratios predicted by the extended isobar model are shown to be in fair agreement with the data, but there are significant differences. The c.m. momentum distributions are also in fair agreement with the predictions of the model, although there are ambiguities in the interpretation. The pion-nucleon Q values give clear evidence for the importance of the $(\frac{3}{2},\frac{3}{2})$ resonant state in multiple pion production, but consideration of this state alone does not provide an explanation of the features of double pion production. Some contribution from another state, possibly the $I=\frac{1}{2}$ nucleon isobar, is necessary. In double production, the c.m. angular distributions of the nucleons show backward-forward peaking suggestive of a one-pion exchange process. The angular distributions of the nucleons from triple production are almost isotropic.

I. INTRODUCTION

THIS is the second of two papers describing the results obtained in an exposure of the BNL 20-in. hydrogen bubble chamber to a 2-Bev scattered-out proton beam at the Cosmotron. Paper I[1] dealt with single-pion production, strange-particle production, and elastic scattering. In this paper, multiple-pion production will be considered, and discussed in terms of the extended isobar model. A similar experiment at 2.85 Bev has been carried out by the BNL Bubble Chamber group.[2] Previous experimental information[3] has been limited by statistics.

II. EXPERIMENTAL DETAILS AND ANALYSIS

The experimental details and analysis procedure have been given in I.

Nine hundred four-pronged events were measured and kinematically analyzed with the GUTS[4] program for the following interpretations:

$$\begin{aligned} p+p &\rightarrow p+p+\pi^+ +\pi^-, && (pp+-)\\ &\rightarrow p+n+\pi^+ +\pi^+ +\pi^-, && (pn++-)\\ &\rightarrow p+p+\pi^+ +\pi^- +\pi^0, && (pp+-0)\\ &\rightarrow d+\pi^+ +\pi^+ +\pi^-,\\ &\rightarrow d+\pi^+ +\pi^+ +\pi^- +\pi^0. \end{aligned}$$

The χ^2 distribution for the $pp+-$ events is shown in Fig. 1(a). It should be noted that this is a four-constraint fit, so that the theoretical distribution is identical with that for elastic pp events. The reactions $pn++-$ and $pp+-0$ give one-constraint fits, and the χ^2 distributions [Fig. 1(b)] are similar to those for the single-pion-production events.

Figures 2(a–c) indicate the missing mass distributions for the $pp+-$, $pp+-0$, and $pn++-$ events, respectively. The distributions are compatible with the measuring errors.

All secondary tracks were identified by ionization, either visually or by bubble counting when necessary.

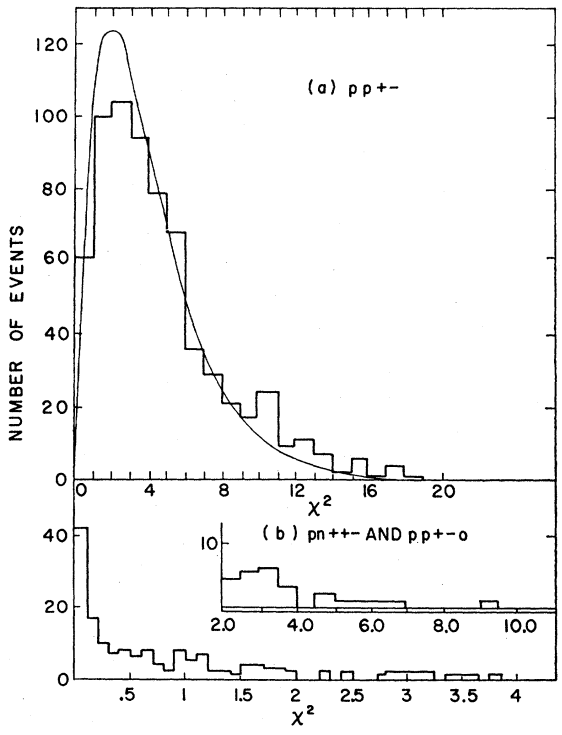

FIG. 1. (a) χ^2 distribution for the reaction $pp+-$. The curve shows the theoretical distribution for four constraints. (b) χ^2 distribution for $pn++-$ and $pp+-0$. The curve is the theoretical distribution for one constraint.

* Work performed under the auspices of the U. S. Atomic Energy Commission.

† On leave of absence from the National Research Council, Ottawa, Ontario, Canada.

[1] W. J. Fickinger, E. Pickup, D. K. Robinson and E. O. Salant, preceding paper [Phys. Rev. **125**, 2082 (1962)].

[2] E. L. Hart, D. Leurs, R. I. Louttit, T. W. Morris, W. J. Willis, and S. S. Yamamoto, Phys. Rev. (to be published).

[3] W. B. Fowler, R. P. Shutt, A. M. Thorndike, W. L. Whittemore, W. T. Cocconi, E. Hart, M. M. Block, and E. M. Harth, Phys. Rev. **103**, 1484 (1956).

[4] J. P. Berge, F. T. Solmitz, and H. Taft, University of California Radiation Laboratory Report UCRL-9097, 1960 (unpublished).

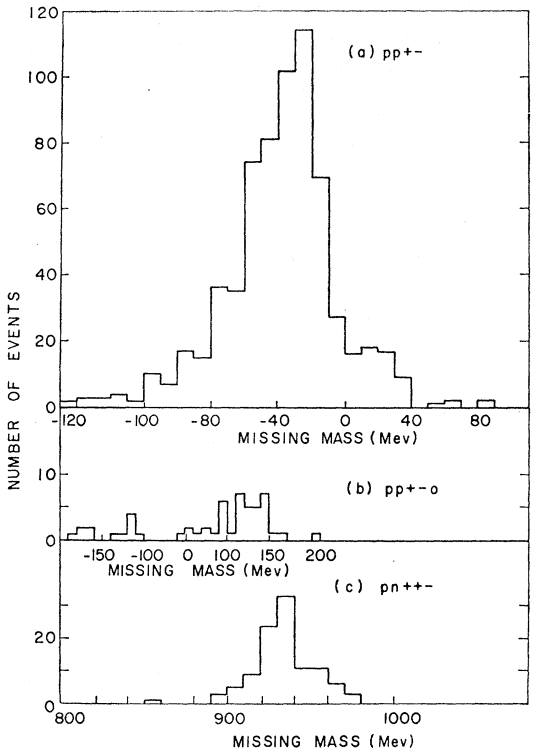

FIG. 2. Missing mass distribuitons for (a) $pp+-$, (b) $pp+-0$, (c) $pn++-$.

Eight six-pronged events were observed in the total sample of 57 300 p-p interactions, but examination showed that these were all of the type $pp+-0$ with a Dalitz pair.

Events of the types

$$\begin{aligned} p+p &\rightarrow p+n+\pi^+ +\pi^0, \quad (pn+0) \\ &\rightarrow p+p+\pi^0+\pi^0, \quad (pp00) \\ &\rightarrow n+n+\pi^+ +\pi^+, \quad (nn++) \end{aligned}$$

were obtained as rejects (events with large χ^2) from the kinematic fitting program for the two-pronged events. Some contamination of these categories is expected from additional π^0 production. In the identification of the events, kinematic limitations on the momenta of particles and Q values of pairs of particles were taken into account, as well as the calculated missing masses.

III. PARTIAL CROSS SECTIONS

Table I shows the numbers of events in each category, and the partial cross sections expressed in terms of the total p-p cross section, which was obtained from bubble chamber track counting, as reported in I. In order to obtain a large sample, the four-pronged events were obtained from a more extensive scan of the bubble chamber pictures, and the cross sections for two- and four-pronged events have been adjusted accordingly. The errors quoted are statistical only. The elastic and single-pion-production cross sections reported in paper I are also given in this table.

It may be noted that, at this energy, the cross section for producing four pions is zero or very small.

Since all relevant cross sections are available, it is possible to compare the results with the predictions of the extended isobar model.[5] On this model it is assumed that multiple (2 and 3) pion production takes place only through the following three channels.

$$p+p \rightarrow 2N_1^* \quad (2N_1^*) \qquad (1)$$
$$\searrow \; 2(N+\pi),$$

$$\rightarrow N+N_2^* \quad (N+N_2^*) \qquad (2)$$
$$\searrow \; N_1^*+\pi$$
$$\searrow \; N+\pi,$$

$$\rightarrow N_1^*+N_2^* \quad (N_1^*+N_2^*)_d \qquad (3)$$
$$\searrow \quad \searrow$$
$$N+\pi \quad N+\pi,$$

where the isobars N_1^* and N_2^* are excited states of the nucleon corresponding to the $I=\frac{3}{2}$ resonance at a total energy in the π-p system 1.23 Bev, and to the $I=\frac{1}{2}$ resonances at 1.51 Bev (N_{2a}^*) and 1.68 Bev (N_{2b}^*).

The sum of the peak values of the N_1^* and N_{2a}^* masses is 2.74 Bev, which is slightly above the total energy, 2.70 Bev, available in the center of mass at incident energy 2 Bev. However, simultaneous excitation of these two states below the peaks may be possible. The process $2N_2^*$ is not considered here since the center-of-mass energy is too small for any significant excitation. On the isobar model, triple production occurs only

TABLE I. Observed partial cross sections.

Reaction	Number of events (not corrected)	σ (mb)[a]	$\Delta\sigma$ (mb)
pp (elastic)	1493	19.21	0.48
$pp0$	318	3.85	0.22
$pn+$	1326	16.06	0.44
$pp+-$	681	2.51	0.14
$pp00$	76	0.92	0.10
$pn+0$	336	4.07	0.21
$nn++$	51	0.62	0.083
$pp+-0$	59	0.217	0.029
$pn++-$	110	0.405	0.040
$pp+-+-$	0[b]	$\lesssim$0.0007	
$pp+-00$	2	$\lesssim$0.005	
$d++-$ and $d++-0$	15	0.055	0.014

[a] Cross sections for $pp00$, $pn+0$, and $nn++$ are uncorrected for triple-pion production with an additional neutral pion.
[b] Out of 57 300 p-p interactions.

[5] R. M. Sternheimer and S. J. Lindenbaum, Phys. Rev. **123**, 333 (1961).

through the cascade process

$$\begin{array}{lll} p+p \rightarrow N_1^*+N_2^* & & (N_1^*+N_2^*)_t \\ \quad\searrow \quad\quad \searrow & & \\ \quad N+\pi \quad N_1^*+\pi & & (4) \\ \quad\quad\quad\quad \searrow & & \\ \quad\quad\quad\quad N+\pi. & & \end{array}$$

The model predicts the ratios of the cross sections for the various double-pion-production modes, and for the triple-pion modes, in terms of the cross sections for the above basic reactions. For the production of two pions the isobar equations are as follows:

$$\sigma(pp+-)=(1/5)\sigma(2N_1^*)+(5/9)\sigma(N_2^*+N)+(1/2)\sigma(N_1^*+N_2^*)_d, \quad (5)$$

$$\sigma(pp00)=(8/45)\sigma(2N_1^*)+(2/9)\sigma(N_2^*+N)+(1/18)\sigma(N_1^*+N_2^*)_d, \quad (6)$$

$$\sigma(pn+0)=(26/45)\sigma(2N_1^*)+(2/9)\sigma(N_2^*+N)+(7/18)\sigma(N_1^*+N_2^*)_d, \quad (7)$$

$$\sigma(nn++)=(2/45)\sigma(2N_1^*)+(1/18)\sigma(N_1^*+N_2^*)_d. \quad (8)$$

Since there are four equations and three unknown quantities the solution is overdetermined, so that calculation of the basic cross sections may be treated as a problem with one constraint. Table II shows measured and calculated double-production cross sections. We have corrected the measured cross sections, $\sigma(pp00)$, $\sigma(pn+0)$, and $\sigma(nn++)$, given in Table I, for triple production by using the measured triple-production cross sections, $\sigma(pn++-)$ and $\sigma(pp+-0)$ and assuming branching ratios predicted by the isobar model. A least-squares fit to the corrected double-production sections, using Eqs. (5)–(8), yielded adjusted values of these cross sections, and the basic isobar cross sections. These are shown in the third column of Table II. This fit gives $\sigma(N_1^*+N_2^*)\simeq\sigma(2N_1^*)$, and a small negative value for $\sigma(N+N_2^*)$, both of which results are unreasonable. By constraining $\sigma(N+N_2^*)$ to be positive we obtained more reasonable values for basic cross sections but the changes required in the measured cross sections were larger. Sternheimer has suggested that adjusting the two smaller experimental cross sections while keeping the two larger ones fixed, and constraining $\sigma(N_1^*+N_2^*)$ to be small might give a more desirable set of values for the basic cross sections. These forced solutions are shown in column 4 of Table II. The adjustments to the smaller cross sections, $\sigma(pp00)$ and $\sigma(nn++)$ are considerably larger than the statistical errors, and larger than reasonable systematic errors in identification. Since the solutions suggest an appreciable contribution from $N_1^*+N_2^*$, and since in this experiment these isobars would be produced at relatively low energies, there is a strong possibility of final-state interaction between the decay particles. No such interference effects are included in the isobar model.

Interference effects occurring in double pion production should also be observed in the triple pion production processes, but there is no evidence for this from the triple-pion branching ratios. The total cross section for the two triple-pion production processes observed, $pn++-$, and $pp+-0$, from $N_1^*+N_2^*$, is about 0.6 mb, which is of the same magnitude as $\sigma(N_1^*+N_2^*)_d$, assumed in fitting the double production cross sections. The ratio $\sigma(pn++-)/\sigma(pp+-0)$ predicted by the model is $25/14=1.79$. The experimental ratio is 1.87 ± 0.32.

TABLE II. Adjusted reaction cross sections and basic isobar cross sections in mb.

Observed reaction	Measured[a]	Least-squares solution	Forced solution
$pp+-$	2.51 ± 0.14	2.51	2.51
$pp00$	0.89 ± 0.10	0.93	1.38
$pn+0$	3.88 ± 0.21	3.88	3.88
$nn++$	0.60 ± 0.08	0.40	0.29
Isobar mode			
$\sigma(2N_1^*)$		4.22	5.40
$\sigma(N_1^*+N_2^*)$		3.78	1.0
$\sigma(N+N_2^*)$		-0.13	1.67

[a] These cross sections for $pp00$, $pn+0$, and $nn++$ have been corrected for triple-pion production as explained in the text.

While the forced solution discussed above is not compatible with all the measured cross sections, the relative proportion of $N+N_2^*$ and $N_1^*+N_2^*$ in this solution seems more reasonable than for the least-squares solution, since the former favors the combination $N+N_2^*$ which requires less center-of-mass energy. In discussing the influence of the $I=\frac{1}{2}$ states on the momentum distributions, the proportion of $N+N_2^*$ given by the forced solution is used, although the failure of the least-squares fit implies some doubt as to the validity of the isobar cascade model.

IV. MOMENTUM DISTRIBUTIONS AND Q VALUES

(a) Double-Pion Production

Figures 3–6 show the momentum distributions for the observed nucleons and pions from the four double production reactions, $pp+-$, $pn+0$, $pp00$, and $nn++$. The pion spectra from $pp+-$ (Fig. 3) show a difference between the negative and positive pions, negative pions being produced at a higher average momentum than positive pions. This difference immediately implies that $2N_1^*$ cannot be the sole mechanism, since $2N_1^*$ alone would require identical pion spectra (long dashes). The significant excess of negative pions at the high-momentum end of the spectrum can be satisfactorily accounted for by adding a contribution from $N+N_2^*$ (solid curve) in the proportions suggested by the basic isobar cross sections (column 4 of Table II) given in Sec. III. The theoretical curves in these and the following figures were obtained by extrapolating the basic isobar curves for 3 and 2.3 Bev to 2 Bev.[5] The contribution from $N_1^*+N_2^*$ has not been included, since the basic curves

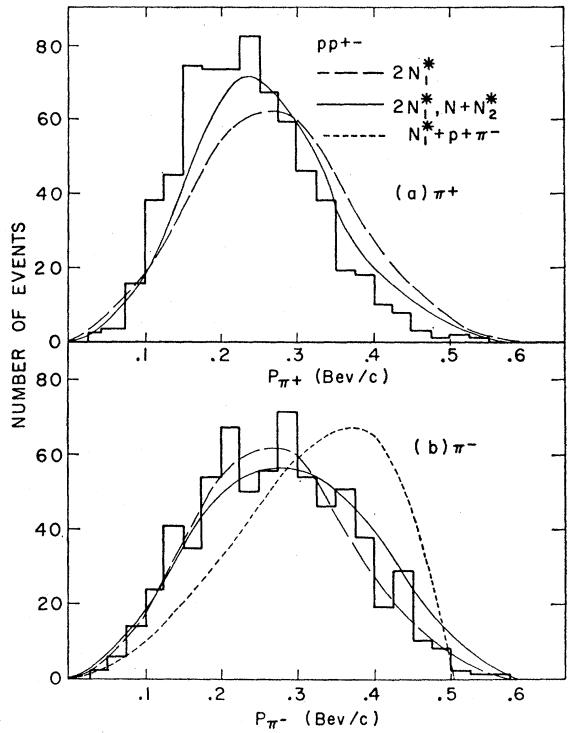

FIG. 3. Center-of-mass momentum spectrum of the pions from $pp+-$. The long-dashed curves are calculated from the isobar model for the production of $2N_1^*$ alone. The solid curves include a contribution from $N+N_2^*$ with $\sigma(2N_1^*)=5.40$ mb and $\sigma(N+N_2^*)=1.67$ mb. The short dashes show a three-body phase-space curve for pions produced statistically in the process $p+p \rightarrow N_1^*+p+\pi^-$.

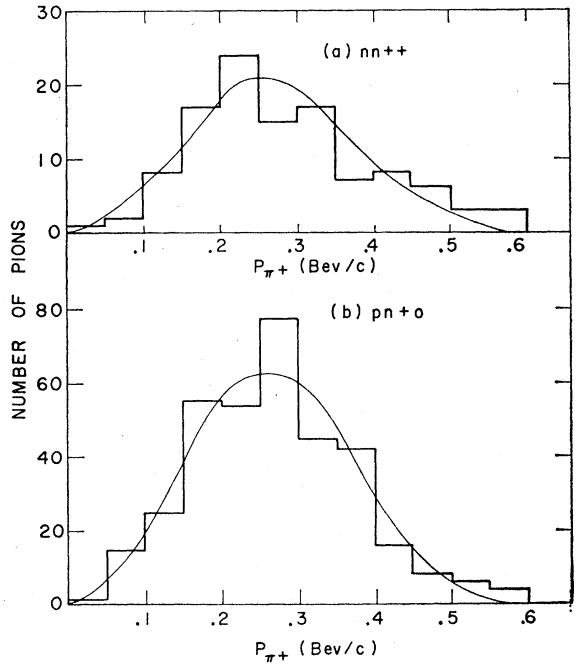

FIG. 4. (a) Center-of-mass momentum distribution of pions from $nn++$. The curve shows the distribution from $2N_1^*$ alone. (b) Center-of-mass momentum distribution of positive pions from $pn+0$.

were not available. The magnitude of the contribution from $N_1^*+N_2^*$ would be comparable with that from $N+N_2^*$. In the $N_1^*+N_2^*$ mode, the isobars would be produced essentially at rest, and contribute positive pions grouped around 210 Mev/c and negative pions around 440 Mev/c. This would still be consistent with the difference between the two experimental distributions.

The short-dashed curve on Fig. 3(b) is a three-body phase-space curve calculated on the assumption that all pions are produced by the reaction

$$\begin{array}{l} p+p \rightarrow N_1^*+p+\pi^- \\ \qquad\quad \searrow \\ \qquad\quad p+\pi^+. \end{array} \tag{9}$$

N_1^* was given a fixed mass of 1.23 Bev. If this process were important the smaller contribution to the negative pion spectrum from

$$\begin{array}{l} p+p \rightarrow N^*+p+\pi^+ \\ \qquad\quad \searrow \\ \qquad\quad p+\pi^- \end{array} \tag{10}$$

would have to be taken into account. If we included this effect, and the effect of the finite width of the isobar mass, the spectrum would still have a maximum around 375 Mev/c, which is clearly incompatible with the data. A mixture of this statistical production [Eqs. (9) and (10)] with $2N_1^*$ [Eq. (1)] might reproduce the experimental pion spectrum.

The positive pion momentum distribution from $pn+0$ [Fig. 4(b)] is not sensitive to effects from the N_2^* isobar. The pion momentum distribution from $nn++$

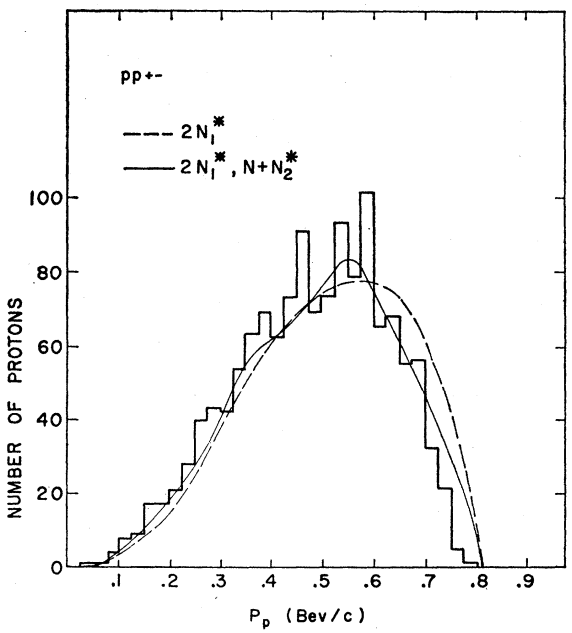

FIG. 5. Center-of-mass momentum distribution of protons from $pp+-$. The dashed curve shows the distribution predicted from $2N_1^*$ and the solid curve, that from $2N_1^*$ and $N+N_2^*$.

[Fig. 4(a)] can only come from $2N_1^*$ or $N_1^*+N_2^*$, and the distribution would be sensitive to an appreciable contribution from $N_1^*+N_2^*$. The solid curve shows the distribution expected from $2N_1^*$ alone. There is a slight indication of the additional effects expected from the $N_1^*+N_2^*$ mode, but statistics are inadequate.

The histogram in Fig. 5 shows the momentum distribution of protons from $pp+-$. The dashed curve shows the distribution predicted from $2N_1^*$, and the solid curve that from $2N_1^*$ and $N+N_2^*$. The solid curve agrees with the data somewhat better than the dashed curve. Inclusion of the $N_1^*+N_2^*$ contribution should further increase the agreement by reducing the average proton momentum. However, an admixture of the statistical process considered for the pions might also explain the data.

The proton distributions from $pp00$ and $pn+0$ are shown in Figs. 6(a) and (b), with theoretical curves for $2N_1^*$ (dashed) and $2N_1^*$ and $N+N_2^*$ (solid) for comparison. For $pp00$ the latter curve is slightly better. For $pn+0$ the observable distributions are dominated by the $(\frac{3}{2},\frac{3}{2})$ isobar, and are not sensitive to the effect of the $I=\frac{1}{2}$ states.

Figure 7 shows Q values for the various possible combinations of nucleons and pions in the $pp+-$ reaction, where Q is the total kinetic energy in the rest frame of the particles considered. The distribution for $p+$ in Fig. 7(a) shows a striking peak at 145 Mev corresponding to the $(\frac{3}{2},\frac{3}{2})$ pion-nucleon resonance. It should be noted that both protons have been used in plotting this distribution although only one is associated with the $p+$ isobar for a given event. The three-body Q value, Q_{p+-}, is shown in Fig. 7(b). The distribution is broad with possible indications of a double maximum corresponding to the two $I=\frac{1}{2}$ resonances, N_{2a}^* at total c.m. energy or isobar mass 1.51 Bev and N_{2b}^* at 1.68 Bev. This may be evidence for the $N+N_2^*$ mode, which should account for about 20% of the distribution if the basic cross sections in column 4 of Table II are correct. Figure 7(c) shows the distribution of Q_{p-}. The peak at 145 Mev corresponding to N_1^* is again evident. If the process $N_1^*+N_2^*$ occurs there should also be a high-energy group from N_2^* (about 10% of the events according to the basic cross sections). Comparison of the Q_{p+} and Q_{p-} distributions shows that there is a high-energy grouping in the latter, which could be consistent with some $N_1^*+N_2^*$. Angular correlations between pairs of particles from the $pp+-$ reaction are shown in Fig. 8.

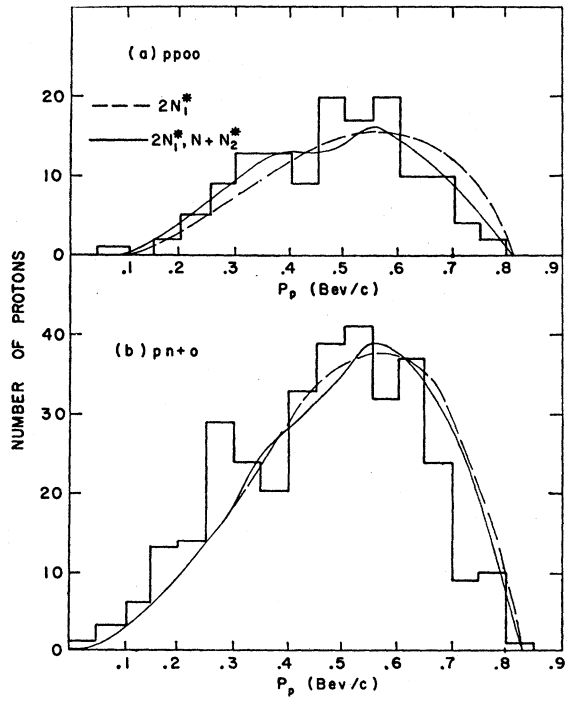

FIG. 6. Center-of-mass momentum distribution of protons; (a) from $pp00$ and (b) from $pn+0$. The dashed curve is for $2N_1^*$; the solid curve is for $2N_1^*$ and $N+N_2^*$.

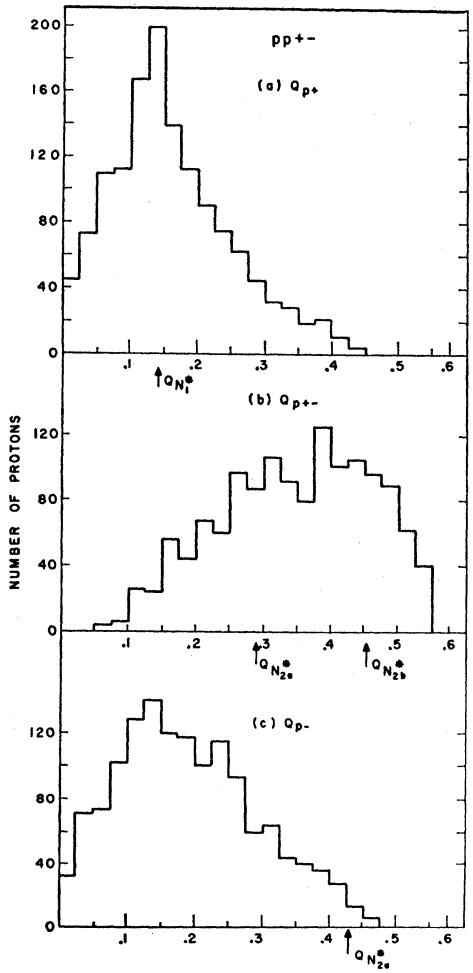

FIG. 7. Pion-nucleon Q-value distribution from $pp+-$.

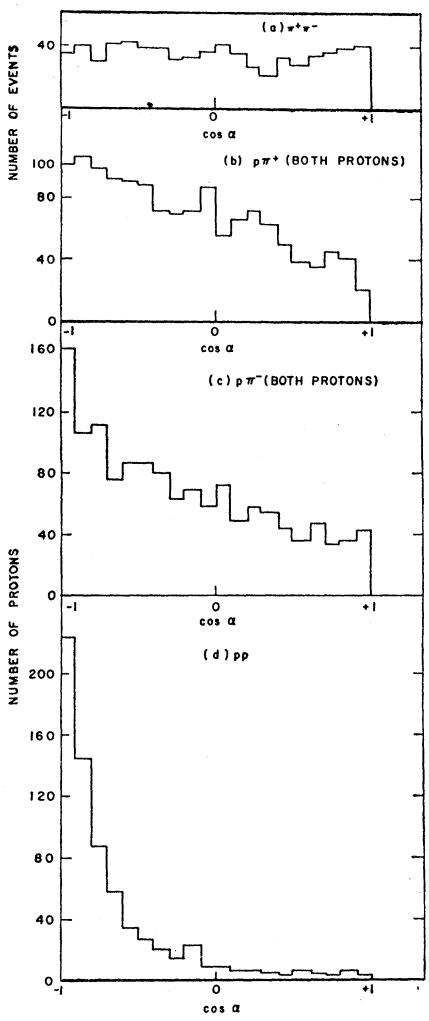

FIG. 8. Center-of-mass angular correlations between pair of particles from $pp+-$.

Figure 9 gives Q_{p+} from $pn+0$. The peak corresponding to the $(\frac{3}{2},\frac{3}{2})$ resonance is clearly visible. It may be noted that, since these events involve the production of two neutral particles, they could not be kinematically fitted, and the Q values are calculated from unadjusted, measured quantities.

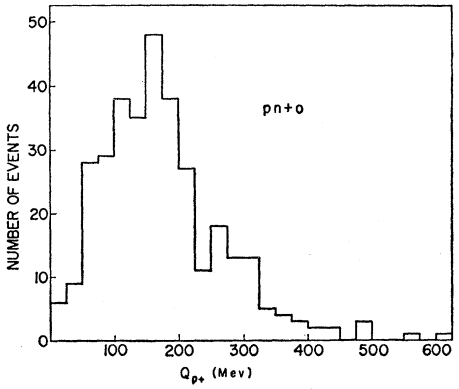

FIG. 9. Q_{p+} distribution from $pn+0$.

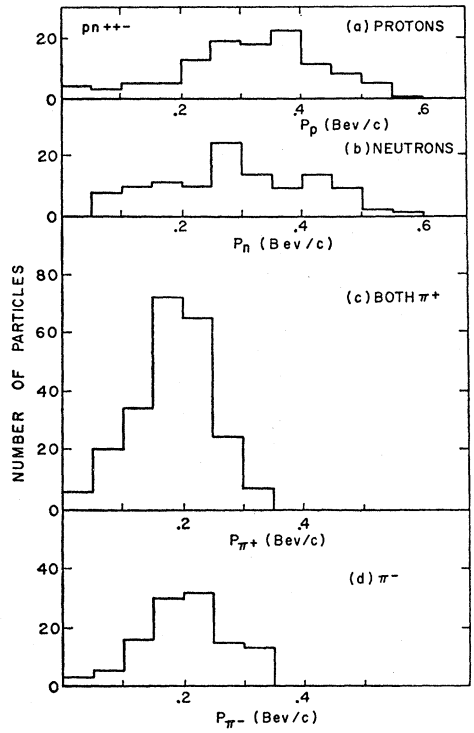

FIG. 10. Nucleon and pion momentum distributions from $pn++-$.

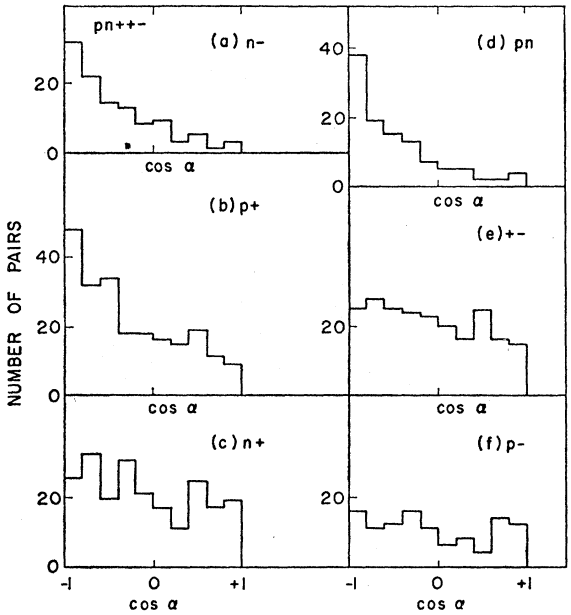

FIG. 11. Center-of-mass angular correlations between pairs of particles in $pn++-$.

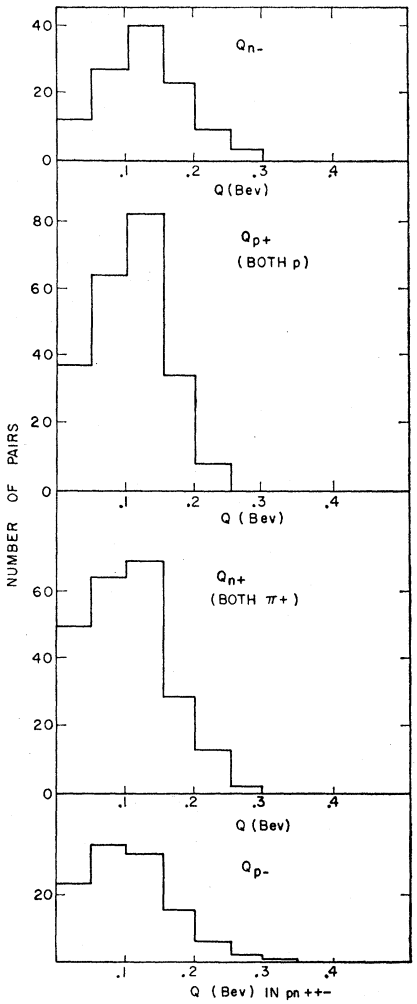

FIG. 12. Two-body pion-nucleon Q values from $pn++-$.

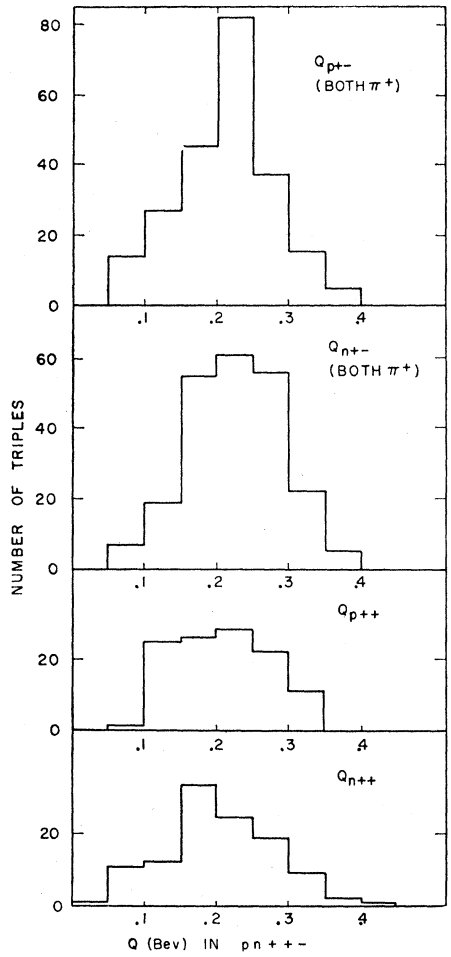

FIG. 13. Three-body (nucleon+2 pions) Q values from $pn++-$.

(b) Triple-Pion Production

Triple production on the isobar model at 2 Bev can come only from the mode $(N_1^*+N_2^*)_t$ [Eq. (4)] with the subsequent cascade decay of N_2^* into two pions. Two combinations, $n+$ and $p+-$ or $p+$ and $n+-$, are possible for the $N_1^*+N_2^*$ with relative weights of 1 to 9. We would then expect to see marked effects from the pure $(\frac{3}{2},\frac{3}{2})$ states, $p+$ and $n-$, in the two-body Q values. Similarly, for the three-body Q values, we would expect to see a strong effect from $n+-$, a weak effect from $p+-$, and no effects from $n++$ and $p++$.

The nucleon and pion momentum distributions from $pn++$ are given in Fig. 10. Both negative and positive pion spectra peak around 200 Mev/c consistent with the decay of slow N^* isobars. Since the available c.m. energy is about 40 Mev below the peak threshold for exciting both N_1^* and N_2^*, the isobars, if produced, would be slow. This is indicated in Fig. 11, which shows the angles between pairs of particles in the c.m. system. There is obvious correlation between the proton and the positive pion, and the neutron and negative pion. Figure 12 shows the two-body pion-nucleon Q values, and Fig. 13 the three-body Q values for the $pn++-$ reaction. The effects of the $(\frac{3}{2},\frac{3}{2})$ resonance are clearly visible in the two-body Q's. The Q_{n++} and Q_{p++} do not show any marked effects, while there are indications of peaks at about 230 Mev for Q_{n+-} and Q_{p+-}. It should be noted that, for each event, there is an ambiguity in the choice of the positive pion. Both possibilities are plotted. The Q distributions and angle correlations show that practically all the protons and neutrons are associated with the $(\frac{3}{2},\frac{3}{2})$ isobar. Evidence for the intermediate formation of a higher isobar is ambiguous.

Figure 14 shows the momentum distributions for the nucleons and pions from the triple production reaction $pp+-0$; Fig. 15 shows two- and three-body Q values. For this reaction there are two possible intermediate states on the isobar picture, $(p+)$ and $(p-0)$, and $(p0)$ and $(p+-)$, which would be in the ratio 9:5. About half (27/56) of the protons should be associated with

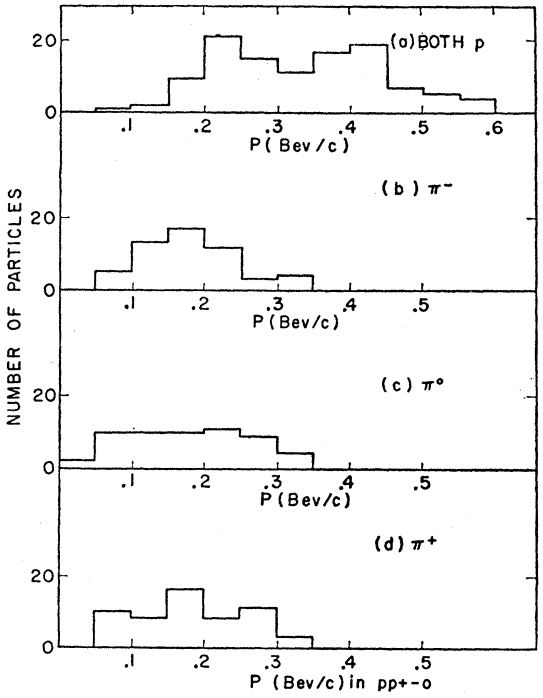

FIG. 14. Center-of-mass momentum distribution of pions and nucleons from $pn+-0$.

positive pions in the $(\frac{3}{2},\frac{3}{2})$ state. The data are inconclusive, perhaps due to the limited statistics. The three-body Q values show no striking characteristics.

The two-pion and three-pion Q values for reactions $pp+-$, $pn++-$, and $pp+-0$ are shown in Fig. 16. There is no evidence that the known two-pion and three-pion resonances at Q values of[6] 475 and[7] 370 Mev, respectively, play a significant part in the interactions. All the two-pion Q distributions show an accumulation of events at low Q values. The three-pion Q distributions $++-$ and $+-0$, Figs. 16(d) and (h), appear to be different, but, because of the poor statistics, it is unjustifiable to draw any firm conclusion about the possibility of a low-energy $I=0$ resonant state in the $pp+-0$ reaction.[8,8a]

[6] E. Pickup, D. K. Robinson, and E. O. Salant, Phys. Rev. Letters **7**, 192 (1961).

[7] B. C. Maglić, L. W. Alvarez, A. H. Rosenfeld, and M. L. Stevenson, Phys. Rev. Letters **7**, 178 (1961).

[8] J. J. Sakurai, Nuovo cimento **16**, 388 (1960).

[8a] *Note added in proof.* Since the $pp+-0$ events showed a Q peak in the position expected for the η meson, a larger sample of four-pronged events was measured. The existence of a three-pion resonance (n) in the $(+-0)$ system with $Q_{+-0}=135$ Mev (mass $=550$ Mev) has been established, confirming the results of Pevsner, *et al.* [A. Pevsner, R. Kraemer, M. Nussbaum, C. Richardson, P. Schlein, R. Strand, T. Toohig, M. Block, A. Engler, R. Gessaroli, and C. Meltzer, Phys. Rev. Letters **7**, 421 (1961)]. The width of the Q peak is approximately equal to the experimental resolution (± 10 Mev), and the height is about four standard deviations above background. Since no corresponding peak appears in the $(++-)$ system in the $pn++-$ reaction, this indicates isotopic spin $I=0$ for the resonance. The cross section for $p+p\rightarrow p+p+\eta$; $\eta\rightarrow\pi^++\pi^-+\pi^0$ was found to be 0.55 ± 0.012 mb.

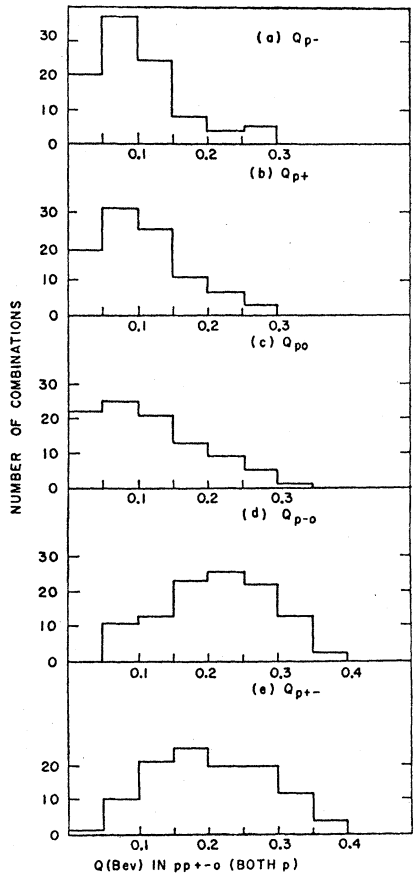

FIG. 15. Two- and three-body pion-nucleon Q values from $pp+-0$.

V. c.m. PRODUCTION ANGLES

Figure 17 shows the c.m. angular distributions of the nucleons from double- and triple-pion production. The distributions from the double production reactions $pp+-$, $pn+0$, and $pp00$ are strongly peaked backward and forward. They are similar to the nucleon distributions in single-pion production, discussed in I. In the single-pion-production processes 46% of the nucleons were in the wings $(0.9<|\cos\theta|<1)$, whereas in the double-production processes only 27% of the nucleons are in the wings. For triple production the distributions are almost isotropic. There may be a slight excess in the wings.

The backward-forward peaking, indicating low four-momentum transfers, implies that the one-pion exchange mechanism is important in double pion production. The $pp+-$ process might proceed through either of the two diagrams shown in Fig. 18.[9,10] Figure 18(a), where the two pions are produced at opposite vertices, could correspond to formation and subsequent decay of $2N_1^*$ or the less important mode $N_1^*+N_2^*$, or to charged pion elastic scattering at the two

[9] S. D. Drell, Phys. Rev. Letters **5**, 342 (1960).

[10] F. Salzman and G. Salzman, Phys. Rev. Letters **5**, 377 (1960).

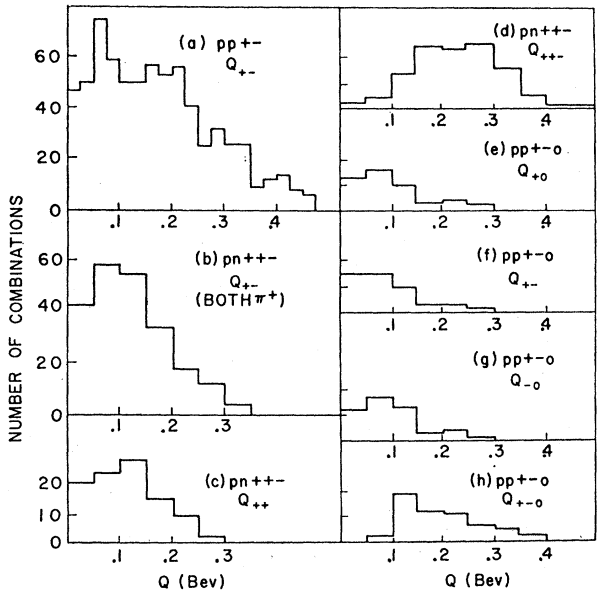

FIG. 16. Two- and three-pion Q values from $pp+-$, $pn++-$, and $pp+-0$.

vertices. Figure 18(b) could correspond to the production and cascade decay of N_2^* at the second vertex, or to inelastic $\pi^0 p$ scattering.

In calculating the theoretical isobar momentum distributions (given in Sec. IV) possible effects of $N_1^* + N_2^*$ were ignored, since the available energy was insufficient for peak excitation of both resonances. On the one-pion exchange model the effect of the $I=\frac{1}{2}$ cross section would be included by using the experimental $\pi^- - p$ elastic scattering cross sections at the second vertex [Fig. 18(a)] with no detailed consideration of pion production through nucleon excitation being necessary. Thus a satisfactory explanation might be given by considering only the mechanism shown in Fig. 18(a), at least for those events in which the four-momentum transfers are small.

This view is supported by the proton c.m. momentum distributions shown in Fig. 19, where the protons have been separated into groups, (a) $|\cos\theta_p| < 0.90$ and (b) $|\cos\theta_p| \geq 0.90$. The distribution of Fig. 19(b) shows no marked evidence of recoils from either of the two $I=\frac{1}{2}$ resonances (N_{2a}^* and N_{2b}^*), thus indicating that the diagram of Fig. 18(b) does not represent the dominant mechanism for this group of events. However, the mechanism of Fig. 18(a) (which could be $2N_1^*$) would favor the production of high-momentum protons. The experimental proton distribution in Fig. 19(b) has a maximum about 620 Mev/c, and is in approximate agreement with the distribution expected from the $2N_1^*$ mode (dashed curve).

The other group of protons has a lower average momentum [Fig. 19(a)]. The distributions could be consistent with the inclusion of some contribution from proton recoils from the $N+N_2^*$ mode. Both groups of

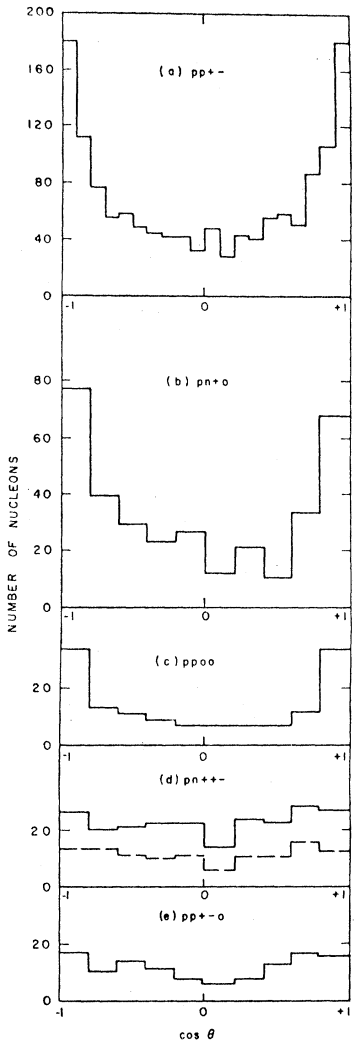

FIG. 17. Center-of-mass angular distributions of nucleons from double- and triple-pion production. In part (d) dashed line corresponds to protons; full line to both nucleons.

events show sharp $p+$ Q values corresponding to the $(\frac{3}{2},\frac{3}{2})$ resonant state.

The c.m. angular distributions of the pions in the $pp+-$ reaction are shown in Fig. 20. The distributions are approximately isotropic, although the negative pion

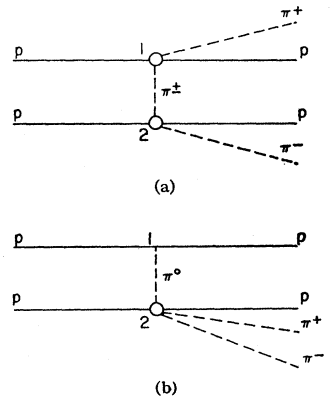

FIG. 18. Diagram showing double-pion production through the one-pion exchange mechanism.

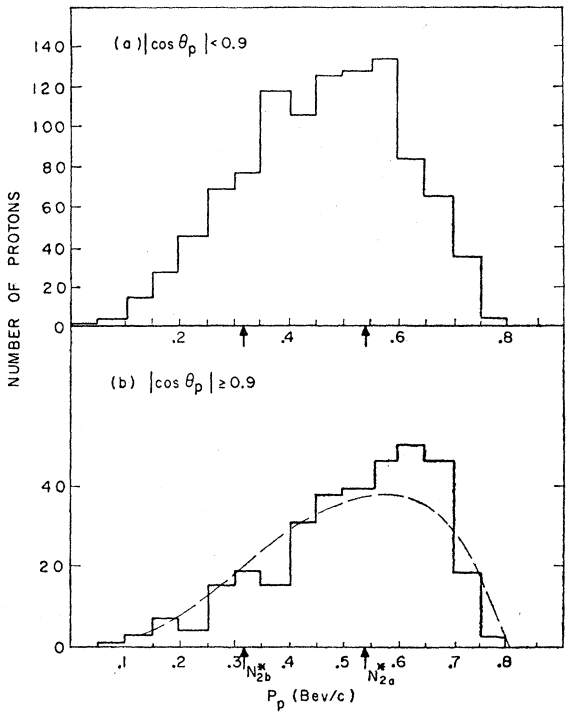

FIG. 19. Center-of-mass momentum distribution of protons from $pp+-$, (a) $|\cos\theta_p| < 0.90$, (b) $|\cos\theta_p| \geq 0.90$, where θ_p is the angle of emission of the proton in the center-of-mass system.

distribution may show slight peaking at the ends of the distribution. The pion distributions from the other double and triple reactions are also approximately isotropic.

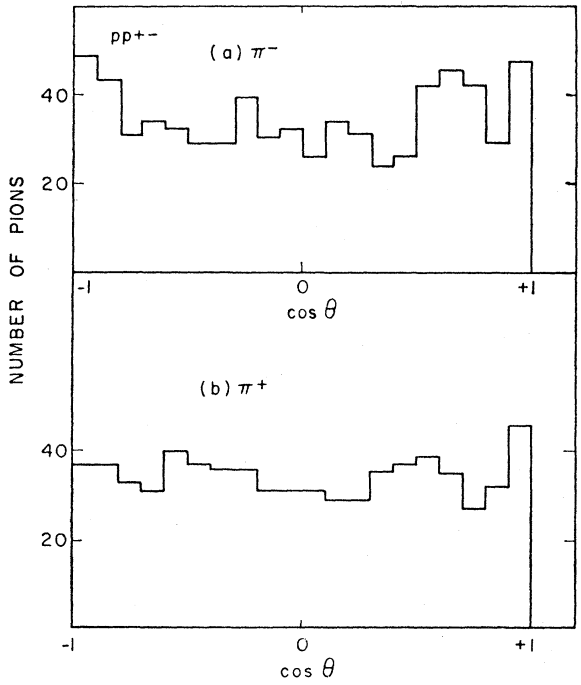

FIG. 20. Center-of-mass angular distributions of pions from $pp+-$.

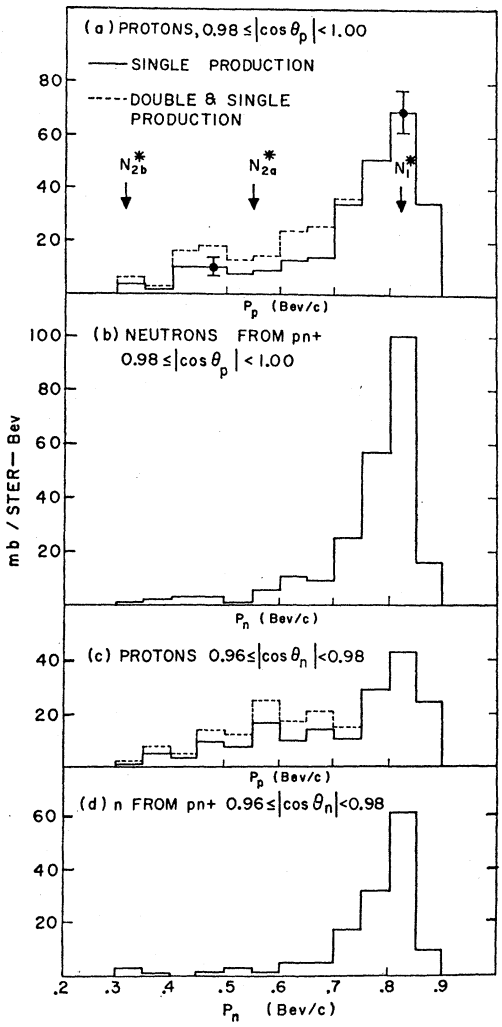

FIG. 21. Center-of-mass momentum distributions of nucleons for single and double pion production at small laboratory angles.

VI. c.m. MOMENTUM DISTRIBUTIONS OF PROTONS FROM SINGLE- AND DOUBLE-PION PRODUCTION AT DIFFERENT LABORATORY ANGLES

It might be of interest to indicate the contributions of protons from the various inelastic processes to the total momentum spectrum for small laboratory angles. Such information may be useful for comparison with counter experiments. Events have been selected with the nucleons in two angular intervals, $|\cos\theta_{c.m.}| \geq 0.98$ corresponding to a mean laboratory angle of $\simeq 2.5°$ for the forward nucleons, and $0.96 < |\cos\theta_{c.m.}| \leq 0.98$ corresponding to a mean laboratory angle of $\simeq 5°$. Figures 21(a) and 21(c) show the distributions for all protons from both single production reactions $pn+$ and $pp0$ (solid line), and for all protons from double as well as single production (dashed line). The contribution of protons from triple production is less than 1 mb/sr Bev. Figures 21(b) and 21(d) show similar distributions for the neutrons from $pn+$.

Double-production processes appear to give a fairly smooth contribution to the cross sections from 300 to 750 Mev/c. The contribution of protons from $pn+$ and $pp0$ in this momentum range is somewhat larger. There is no clear evidence for the effects of the $I=\frac{1}{2}$ resonances, but statistics are small.

VII. CONCLUSIONS

The predictions of the extended isobar model are in approximate agreement with the relative values of the cross sections for the double-pion-production reactions $pp+-$, $pp00$, $pn+0$, and $nn++$, but there are significant discrepancies. The predicted ratio of the two triple production cross sections, $\sigma(pn++-)$ and $\sigma(pp+-0)$ is in agreement with the observed value. The two-body Q values indicate that the $(\frac{3}{2},\frac{3}{2})$ resonance plays an important part in multiple production.

The difference between the momentum distributions for the positive and negative pions from the reaction $pp+-$ shows that double pion production does not take place through the $(\frac{3}{2},\frac{3}{2})$ resonance alone ($2N_1^*$). The c.m. momentum distributions appear to be consistent with the inclusion of effects from the $I=\frac{1}{2}$ resonant states, but they do not provide a rigorous test of the isobar cascade model.

The c.m. angular distributions of the nucleons indicate that the one-pion exchange mechanism may play an important role in double-pion production.

ACKNOWLEDGMENTS

We wish to thank the BNL Bubble Chamber Group, the members of the Cosmotron staff, and our scanners for their invaluable services. We are indebted to Dr. W. J. Fickinger for providing data from his sample of the two-pronged events (paper I), to Dr. R. M. Sternheimer for discussion, and to Yam Chiu for assistance with the computations.